Dynamics of microfluidic droplets

Charles N. Baroud,*[a] Francois Gallaire[b] and Rémi Dangla[a]

Received 19th January 2010, Accepted 28th April 2010
DOI: 10.1039/c001191f

This critical review discusses the current understanding of the formation, transport, and merging of drops in microfluidics. We focus on the physical ingredients which determine the flow of drops in microchannels and recall classical results of fluid dynamics which help explain the observed behaviour. We begin by introducing the main physical ingredients that differentiate droplet microfluidics from single-phase microfluidics, namely the modifications to the flow and pressure fields that are introduced by the presence of interfacial tension. Then three practical aspects are studied in detail: (i) The formation of drops and the dominant interactions depending on the geometry in which they are formed. (ii) The transport of drops, namely the evaluation of drop velocity, the pressure-velocity relationships, and the flow field induced by the presence of the drop. (iii) The fusion of two drops, including different methods of bridging the liquid film between them which enables their merging.

I. Introduction

Interest in manipulating droplets in microchannels has emerged from two distinct but complementary motivations. The first results from the desire to produce well calibrated droplets for material science applications, for example in the pharmaceutical or food industries. In this context, microfluidics provides a way for producing such droplets in a controlled and reproducible manner, also allowing complex combinations to be designed and explored.[1,2] A second motivation originates in lab on a chip applications where drops are viewed as micro-reactors, in which samples are confined, and which offer a way to manipulate small volumes.[3] The idea of performing chemical or biochemical reactions in droplets had already been explored, before the microfluidics era, through the use of emulsions in order to "compartmentalize" reactions inside many small parallel volumes.[4,5] The introduction of microfluidics tools again acts to facilitate the production and manipulation of these compartments.

By the same token, the use of drops addresses one of the most fundamental problems encountered in single-phase microfluidics by providing control over dispersion and mixing of chemicals, through the encapsulation of the analytes within the drop.[3] The

[a]*LadHyX and Department of Mechanics, École Polytechnique, CNRS, 91128 Palaiseau cedex, France. E-mail: baroud@ladhyx.polytechnique.fr*
[b]*Institut de génie mécanique, Sciences et techniques de l'ingénieur, École Polytechnique Fédérale de Lausanne, Switzerland*

Charles N. Baroud

Charles Baroud is Professeur Chargé de Cours *at École Polytechnique in France, where he founded and leads the microfluidics research group at the Laboratoire d'Hydrodynamique (LadHyX). He studied at MIT then at the University of Texas at Austin, before doing a post-doc at École Normale Supérieure in Paris. Since 2002, his microfluidics research focuses on multiphase flows in complex geometries and on the control of droplet microfluidics for lab on a chip applications.*

Francois Gallaire

François Gallaire gained his PhD from the Hydrodynamics Laboratory (LadHyX), École Polytechnique, Paris. A CNRS research fellow at the J.A. Dieudonné Laboratory, Nice Sophia-Antipolis University until 2009 he left to join the École Polytechnique Fédérale de Lausanne (EPFL) as founding professor of the Laboratory of Fluid Mechanics and Instabilities (LFMI). His research into the basic physical mechanisms governing fluid dynamics is guided by real applications. He designs active flow control strategies to dampen instabilities in archetypical detached boundary layer and swirling flows or to enhance them in confined wakes. His contributions to the field of microfluidics include modeling laser manipulation of a droplet in a micro-canal using a depth-averaged set of equations to account for thermocapillary action at the interface.

manipulation of small volumes is also simplified: Indeed, drops provide new physical and chemical contrasts with the outer medium, such as the dielectric constant or interfacial tension, which can be used to manipulate the minute volumes on-chip while bypassing large lab machines.[6] Moreover, they reduce the sensitivity of the devices to the surface properties of the microchannel, since the fluid of interest is isolated from the walls by the carrier phase.

All these advantages however come at the price of raising a new set of fluid dynamical problems that appear due to the deformable interface of the droplets, the need to take into account interfacial tension and its variations, and the complexity of singular events such as merging or splitting of drops. In the physicist's vocabulary, drops introduce nonlinear laws into the otherwise linear Stokes flows. Evidence of this nonlinearity can be found, for example, by considering that different flow regimes can appear in the same channel and under the same forcing conditions.[7] Moreover, small variations of the driving conditions can lead to transitions between the production of drops or of stable jets, a classical signature of nonlinear instabilities.[8,9] These transitions between widely different behaviours are possible because modifications in the drop geometry couple back to the flow profiles and amplify initially small variations.

A large body of work has recently attempted to tackle these fluid dynamical questions, leading along the way to creative new designs for microfluidic systems and new physical approaches to control the behaviour of drops. Below we will discuss this body of literature while concentrating on drops in microfluidic channels. We will avoid any comparison between the behaviour of droplets within closed microchannels and on open patterned surfaces, an approach sometimes called "digital microfluidics". For a comparative study of these two approaches, the reader is referred to the review article by Darhuber and Troian.[10] We will further limit our review to three fundamental aspects of droplet microfluidics: production of droplets, their transport, and their merging. We begin by considering the underlying physical ingredients, before moving on to specific considerations for each operation.

II. Physical ingredients

The main modification that droplets bring to single phase microfluidic flows comes through the introduction of interfacial tension. This new physical ingredient can be thought of in two complementary ways, either of which can be used depending on the point of view to be taken.

First of all, it is a *force per unit length* which pulls the interface with a magnitude γ (N m^{-1}). As such, any spatial imbalance in the value of γ will lead to a flow along the interface from the low to the high interfacial tension regions, a phenomenon known as Marangoni flow. Since the value of the surface tension varies with temperature and with the contamination of the interface by surfactant molecules, either of these can lead to a Marangoni flow, which is then referred to as thermocapillary or solutocapillary flow, respectively.

Interfacial tension can also be thought of as an energy per unit area (J m^{-2}) which acts to minimise the total surface area so as to reduce the free energy of the interface. The minimum area for a given volume is a sphere, which is the shape taken by an isolated droplet or bubble. Confined drops on the other hand must adapt their shape to the presence of walls, while still curving their interface. The curvature introduces a pressure jump, known as the *Laplace pressure*, between the inside and the outside of the droplet. It is written as $\Delta P = \gamma(1/R_1 + 1/R_2)$, where R_1 and R_2 are the two principal radii of curvature of the interface. The pressure jump is determined locally at each position of the interface; since R_1 and R_2 can vary in space, this can induce pressure variations within a droplet. These supplementary pressure variations will play a major role in determining the flow conditions as we shall see further.

From a modeling point of view, the presence of droplets also introduces new kinematic and dynamic boundary conditions on the fluid flow, since the immiscible fluids cannot cross the interface. The first new boundary condition states that the local normal component of the velocities in each fluid must be equal to the interface velocity. Second, the velocities tangent to the interface must also be equal inside and outside the droplet. Third, the tangential shear stresses must also be balanced at the interface when it is clean of contaminants. This means that the variation of the tangential velocity ($u_{\|}$) with respect to the normal direction r, inside ($\partial u_{\|}/\partial r|_{\mathrm{in}}$) and outside ($\partial u_{\|}/\partial r|_{\mathrm{out}}$) the drop, must balance

$$\mu_{\mathrm{in}} \left.\frac{\partial u_{\|}}{\partial r}\right|_{\mathrm{in}} = \mu_{\mathrm{out}} \left.\frac{\partial u_{\|}}{\partial r}\right|_{\mathrm{out}} . \qquad (1)$$

Eqn (1) introduces the importance of the viscosity ratio $\lambda = \mu_{\mathrm{in}}/\mu_{\mathrm{out}}$, which plays a determining role for the flow fields inside and outside a moving drop or bubble. Fourth, the jump in normal stress at the interface leads to a generalization of Laplace's law taking into account the viscous normal stress in addition to the pressure contribution.

A. Dimensionless numbers

As always in fluid dynamics, the fluid behaviour will depend on the values taken by some important dimensionless numbers which compare different physical ingredients. In what follows we will limit ourselves to inertia-less fluid mechanics, meaning that we will consider small Reynolds number regimes. The Weber number (We $= \rho U^2 l/\gamma$ where U represents a characteristic velocity scale), which compares inertia to interfacial tension, will

Rémi Dangla

Rémi Dangla is a PhD student at LadHyX, École Polytechnique, under the supervision of Prof. Charles N. Baroud. His research focuses on droplet dynamics and manipulations in microchannels of high aspect ratio. He received his Masters degree in Fluid Mechanics and his Diplome d'Ingénieur from École Polytechnique, France.

also generally be small in microfluidics. Note however that inertial effects can come into play in certain situations of high-speed flows, for example for high throughput or droplet breakup situations. Finally, we will ignore the effects of gravity, which can be quantified by taking the Bond number, which compares gravity to interfacial tension, to be small: $\mathrm{Bo} = \Delta\rho g l^2/\gamma \ll 1$, where $\Delta\rho$ is the difference in fluid densities, g is the acceleration of gravity, and l a characteristic length scale.

This leaves interfacial tension and viscosity in competition with each other, since both tend to become important at small scales. The relative strength of the two is expressed by the Capillary number $\mathrm{Ca} = \mu U/\gamma$, where μ is generally the larger viscosity acting in the system. A low value of Ca indicates that the stresses due to interfacial tension are strong compared to viscous stresses. Drops flowing under such a condition nearly minimise their surface area by producing spherical ends. In the opposite situation of high Ca, viscous effects dominate and one can observe large deformations of the drops and asymmetric shapes.

In some cases of interest the velocity varies over a length scale different from the radius of the drop, for example when the channel geometry expands or contracts. In this case, a new capillary number emerges, based on the characteristic magnitude of the shear stress inherent to the flow $\mu dU/ds$, where s represents a spatial direction. These stresses must still be compensanted by the Laplace pressure, which yields $\mathrm{Ca}_s = \mu(dU/ds)R/\gamma$. This capillary number describes the magnitude of deformation observed on a drop due to variations in velocity,[11] for example as a drop enters a bifurcating microchannel.[12,13]

B. Surfactant effects

The value of interfacial tension displays a strong dependence on the local surface coverage with surfactant molecules. These molecules are often added on purpose, in order to facilitate the creation and transport of drops, but can also appear as impurities in the fluids or as by-products of chemical reactions. As such, the value of interfacial tension can vary spatially if the surface concentration displays spatial variations. This has an important consequence as it introduces a tangential stress jump in eqn (1), called Marangoni stress,

$$\mu_{\mathrm{in}} \left.\frac{\partial u_{\parallel}}{\partial r}\right|_{\mathrm{in}} = \mu_{\mathrm{out}} \left.\frac{\partial u_{\parallel}}{\partial r}\right|_{\mathrm{out}} + \nabla_{\parallel}\gamma \qquad (2)$$

where $\nabla_{\parallel}$ indicates the derivative along the tangent to the interface at every point. For clean and isothermal interfaces, one recovers eqn (1). The relation between γ and the local surfactant concentration is nonlinear, sometimes modelled through the so-called "Langmuir model".[14]

A complete description of surfactant transport is beyond the scope of this review but one can readily see that these molecules can be transported either by the hydrodynamic flow (advection), or through molecular diffusion, either in the bulk or along the interface.[15,16] In addition to their transport, surfactants are characterised by several physico-chemical constants: (i) the partition coefficient, which measures the relative bulk and surface concentrations at equilibrium, as well as (ii) their adsorption and desorption rates on the interface, which measure the chemical kinetics. Finally, any change in the shape of a drop will lead to local contraction or expansion of the interface, which lead to an increase or a decrease, respectively, of surface concentration.

All of the above mechanisms can lead to variations of interfacial tension along the drop surface, which will couple back with the drop formation and motion, in addition to influencing droplet fusion. Since different surfactant molecules have different characteristics, changing surfactants can have a major impact in drop behaviour regarding the areas covered in this review. In this regard, stationary model experiments, such as the pendant drop method for measuring surface tension, can help guide the physical understanding. Practical microfluidics situations however often involve a complex interplay between several effects which cannot be simply described in intuitive terms.

III. Droplet production in microchannels

The first step in the microfluidic life cycle of a droplet is its production. Besides a few implementations of the drop-on-demand technique based on the control of integrated microvalves, the majority of microfluidic methods produce droplet volumes ranging from femtolitres to nanolitres. This is achieved through passive techniques which generate a uniform, evenly spaced, continuous stream.[17] These strategies take advantage of the flow field to deform the interface and promote the natural growth of interfacial instabilities, thus avoiding local external actuation. Droplet polydispersity in these streams, defined as the standard deviation of the size distribution divided by the mean droplet size, can be as small as 1–3%.

Not only should devices for making drops produce a regular and stable monodisperse droplet stream, they also need to be flexible enough to provide droplets of prescribed volume at a prescribed rate. To this end, three main approaches have emerged based on different physical mechanisms; they are best described by the flow field topology in the vicinity of the drop production zone: (i) breakup in co-flowing streams (Fig. 1), (ii) breakup in cross-flowing streams (Fig. 2) and (iii) breakup in elongational strained flows (Fig. 3).

In all three cases, the phase to be dispersed is driven into a microchannel, where it encounters the immiscible carrier fluid which is driven independently. The junction where the two fluids meet is designed to optimize the reproducibility of droplet production. Indeed, the geometry of the junction, together with the flow rates and the physical properties of the fluids (interfacial tension, viscosities) determine the local flow field, which in turn deforms the interface and eventually leads to drop/bubble pinch off. The size of the droplet is set by a competition between the

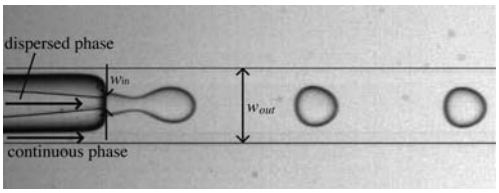

Fig. 1 Example of droplet production in a co-axial injection device. The inner flow is produced by a thin round capillary and enters into a square capillary.

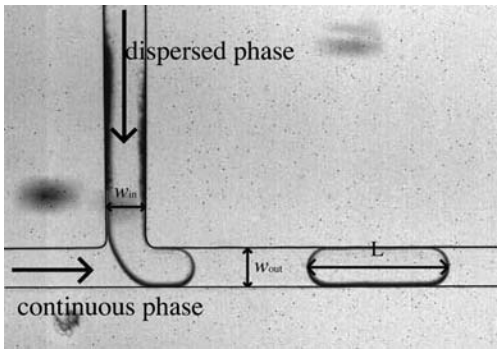

Fig. 2 Example of droplet production in a T-junction. The dispersed phase and the carrier phase meet at 90 degrees in a T-shaped junction.

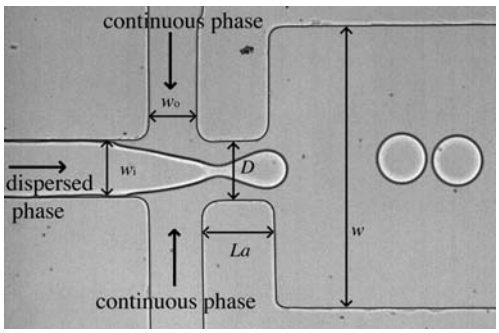

Fig. 3 Example of droplet production in a flow-focusing device. The dispersed phase is squeezed by two counter-streaming flows of the carrier phase, forcing drops to detach.

pressure due to the external flow and viscous shear stresses, on the one hand, and the capillary pressure resisting deformation on the other.

Among all dimensionless numbers, the most important is therefore the capillary number Ca based on the mean continuous phase velocity, which compares the relative importance of the viscous stresses with respect to the capillary pressure. This number ranges between 10^{-3} and 10^{1} in most microfluidic droplet formation devices. Additional dimensionless parameters are the ratio of flow-rates $q = Q_{in}/Q_{out}$, viscosities $\lambda = \mu_{in}/\mu_{out}$, and the geometric ratios, typically the ratio of channel widths $x = w_{in}/w_{out}$.

Below, we review the current understanding regarding the mechanisms at play in each of the three geometries that have come to dominate droplet production. While the physics at the origin of droplet production in co-axial injectors is easily identified as related to the Rayleigh-Plateau instability, the cylindrical geometry of the injector is a serious obstacle to its implementation in soft lithography Lab on the Chip devices. In contrast, the two alternative geometries of T-junction and flow focusing are well suited to planar geometries but present more complex fluid dynamics, as detailed below.

A. Co-flowing streams

A typical example representing the geometry of co-flow devices is shown in Fig. 1. It corresponds to a cylindrical glass tube that is aligned with a square or rectangular outer channel, with the two streams flowing in parallel near the nozzle. It was first implemented in the context of microfluidics by Cramer *et al.*,[18] who inserted a micro-capillary into a rectangular flow cell. They showed that the breakup of the liquid stream into droplets could be separated into two distinct regimes: dripping, in which droplets pinch off near the capillary tube's tip, and jetting in which droplets pinch off from an extended thread downstream of the tube tip. The transition from dripping to jetting occurs when the continuous phase velocity increases above a critical value, U^*. They found that the value of U^* decreases as the flow rate of the dispersed phase increases. U^* was also found to depend on the viscosities of the inner and outer phases, as well as on the interfacial tension.

The trends from ref. 18 were confirmed simultaneously by Utada *et al.*[19,20] and Guillot *et al.*,[8,21] through stability analyses of viscous threads confined within a viscous outer liquid in a microchannel. Both groups interpreted the transition from dripping to jetting as a transition from an absolute to a convective instability, a terminology which refers to the ability of perturbations to grow and withstand the mean advection: Absolute instabilities grow faster than they are advected, contaminate the whole domain and yield a self-sustained well-tuned oscillation. In contrast, convective instabilities are characterised by a dominating advection of the perturbations and behave as amplifiers of the noise that may exist in the system.[9] In co-axial injection devices, an absolutely unstable configuration is expected to result in a self-sustained formation of droplets close to the device inlet, while a convectively unstable flow is expected to result in droplets which form a finite distance downstream, only after the instability has had space to grow.

Using a lubrication approximation, Guillot *et al.*[8] analysed the transition in detail as a function of the viscosity ratio, the capillary number and the equilibrium confinement parameter x, defined as the ratio of the equilibrium jet radius to the effective radius of the square outer channel. For a given confinement parameter, absolute instability was found to exist below a critical value of the capillary number, which is assumed to determine the transition from dripping to jetting. The critical value decreases as the confinement parameter increases and the transition thresholds agree well with the experimental observations, making the interpretation of the dripping/jetting transition as an absolute/convective instability transition appealing. However, to date no experimental verification has been made of the frequency and wavelength selection that follows from the theoretical analysis. Such quantitative comparison would be useful to confirm the stability analysis interpretation.

The theory mentioned above was developed for co-axial streams flowing in a circular cylindrical geometry. However, the authors also considered the influence of the geometry of the outer channel and showed that the instability was suppressed as soon as the inner jet radius increased beyond the smallest half-side of rectangular channels. The stabilization mechanism relies on the fact that a cylindrical thread can decrease its surface area when subjected to a varicose perturbation, while a squeezed, quasi two-dimensional thread always increases its surface when perturbed. This was first observed within the microfluidic context by Migler[22] and further analyzed and applied by Humphry *et al.*,[23]

among others. More recently, Utada *et al.*[20] have generalized these results by relaxing first the lubrication assumption and then the creeping flow limit, thus considering inertial effects that become significant at large capillary numbers.

B. T-junctions

Droplet formation in a T-shaped device was first reported by Thorsen *et al.*,[24] who used pressure controlled flows in microchannels to generate droplets of water in a variety of different oils. A typical example of a T-junction is depicted in Fig. 2, which shows the two phases flowing through two orthogonal channels and forming drops when they meet.

Three regimes could be distinguished as $x = w_{in}/w_{out}$, the ratio of the dispersed phase channel width to the carrier phase channel width, and the flow-rate ratio are varied. When $x \ll 1$ and when the capillary number is large enough, the droplets are emitted before they can block the channel and their formation is entirely due to the action of shear-stress. In this regime, sometimes called the dripping regime, droplets break when the viscous shear stress overcomes the interfacial tension, analogous to spherical droplet breakup. A second regime, the squeezing regime, is observed for x of order 1 and when the capillary number is low enough, as described by Garstecki *et al.*[25] In this case, the droplet obstructs the channel as it grows, restricting the flow of the continuous phase around it. This reduction in the gap through which the continuous phase can flow leads to a dramatic increase in the dynamic pressure upstream of the droplet, thus forcing the interface to neck and pinch off into a droplet. The combined influence of the Capillary number and the viscosity ratio on the transition to this second regime of droplet formation has been analyzed numerically by de Menech *et al.*[26] The squeezing regime further evolves into the formation of stable parallel flowing streams when the dispersed phase flow rate becomes larger than the continuous phase flow rate.[27] The critical dispersed phase velocity required for the transition from droplet formation to parallel flowing streams decreases with an increase in viscosity of the dispersed phase.

With their analysis of the squeezing regime, Garstecki *et al.* predict that the drop length increases linearly with the flow-rate ratio[25] and that the droplet length is independent of the continuous phase viscosity over a wide range of oil viscosities. On the other hand, more recent numerical studies[28] and experimental work[29,30] demonstrate that the viscosity ratio is indeed important for the droplet formation process in the intermediate regime ($x < 1$) where both shear stress and confinement strongly influence the shape of the emerging droplet. Christopher *et al.*[30] further establish an extended scaling law which accounts for the influence of the viscosity and channel width ratios, also proposing scaling laws for the rate of production of droplets, which agree well with the experiments. Most recently Van Steijn *et al.*[31] related the neck collapse to significant reverse flow in the corners between the phase to be dispersed and the channel walls.

C. Flow focusing devices

In the flow focusing geometry, first proposed by Anna *et al.*[32] and Dreyfus *et al.*,[33] the dispersed phase is squeezed by two counter-flowing streams of the continuous phase. Four main regimes can be identified as the parameters are varied: squeezing, dripping, jetting and thread formation. However, the large number of geometrical aspect ratios characterizing flow-focusing devices has prevented the determination of simple scaling laws to predict the droplet size, distribution and rate of emission as a function of the key parameters. Indeed, three new lengths are introduced in the problem in addition to w_{in} and w_{out}, as seen in Fig. 3: the width of the aperture D and its length L_a, as well as the collector channel width w.

Nevertheless, the mechanisms governing squeezing-dripping regime when the dispersed phase is a gas have been studied by Garstecki *et al.*[34] and later by Dollet *et al.*[35] In this squeezing regime, the droplet breakup proceeds in two distinct phases: The squeezed thread begins by thinning down quasi-statically through the effect of the hydrodynamic forcing[34] and the duration of this first phase increases with the aspect ratio of the channel and is absent for square capillaries.[35] Then, as the thread size becomes similar to the depth of channel, it adopts a cylindrical shape and rapidly becomes unstable due to the capillary (Rayleigh-Plateau) instability. The breakup then takes place as classical droplet pinch-off, governed by inertia and surface tension.[35]

It is yet not clear if this scenario for gas threads operates in the same way for the viscous liquid jets described for instance by Cubaud *et al.*[36] or Lee *et al.*[37] In addition to the difference in the viscosity contrast in the two cases, liquid flows are generally forced by controlling the volumetric flow rates while constant pressure is typically used to control the flow of gas. As such, many of the physical arguments used in deriving the droplet scaling laws[34,35] break down. Indeed, Ward *et al.*[38] report a much higher sensitivity of the bubble size to flow rate variations when flow rate rather than pressure is controlled, even though the two parameters are linearly related to each other in a single-phase flow. The details of these differences are complex and not fully explained, although they are attributed to the nonlinearities introduced by surface tension.

As already mentioned, there are no available clear-cut scaling laws for the transitions between various regimes nor for the size and rate of production of droplets. Recent velocity field measurements[39] suggest that the squeezing phenomenon is governed by the build up of a pressure difference as the advancing finger partially blocks the outlet channel, *via* a mechanism very similar to the one active in T-junctions. Other reports however state that squeezing/dripping droplet breakup depends solely on the upstream geometry and associated flow field, and not on the geometry of the channel downstream of the flow focusing orifice.[37] By contrast, the elongation and breakup of the fine thread during the thread formation mode of breakup depends solely on the geometry and flow field in the downstream channel. In light of these recent papers and despite the widespread use of flow-focusing devices, it is clear that the understanding of their detailed dynamics still warrants further research.

D. Active control of droplet production

Applications of droplet microfluidics to Lab on a Chip technologies will eventually require finer and more local control of droplet production than what is allowed by passive techniques. When the fluids are driven with constant flow rates, the volume fraction of the dispersed *vs.* carrier phase is fixed by the ratio of

flow rates. The control of drop formation can therefore only change the frequency and size of drops simultaneously while respecting the volume fraction. In the case when the dispersed flow is controlled by a pressure source, one can block the production of drops for long times and thus vary independently the size and frequency of the droplets.

Control mechanisms for droplet production that rely on integrated micro-valves have been proposed.[40–42] Closer to the topic of this review, variations in drop generation can be produced by varying any of the physical or geometric parameters that enter into the stress balances described in the previous sections. In this context, temperature variations by a localised laser heating have emerged as a useful approach to varying the interfacial tension and thus inducing additional stresses on the drop surface. The Marangoni flows that are produced by the laser heating were shown to block drop formation both in flow-focusing[43] and in T-junction geometries.[6] This method provides a way to actively control the frequency and size of drops, in the case of constant flow rate forcing, and can be used to delay drop formation indefinitely in the case of constant pressure forcing.

Another approach to use heat to modify the production was introduced by Nguyen *et al.*[44] and later used by Stan *et al.*,[45] who tuned the temperature at the flow focusing device through a micro-fabricated heater. By relying on the variations of viscosity and surface tension with temperature, the authors showed significant variations in the size of emitted droplets for fixed flow rate conditions.

IV. Droplet transport

After droplets are produced, they are transported along microfluidic channels by the carrier fluid. The associated two-phase flows have received much interest and can be separated into two limiting categories: (i) bubbly flows for droplets of diameter smaller than the channel size H (Fig. 4A) and (ii) slug flows in the opposite case, where each droplet occupies most of the channel's cross section (Fig. 4B). In the first case, drops are typically assumed to flow at the local velocity of the carrier fluid and will tend to follow the streamlines of the external phase. This implies that drops that are nearer to the channel centreline will flow faster than those close to the edges. Moreover, drops arriving at a bifurcation will take the path that is dictated by the local streamlines of the carrier fluid.[46] In contrast, the second category is more interesting, from a hydrodynamics point of view, because the flow is strongly modified by capillary effects and by the deformability of the drop interfaces. This places the capillary number based on the velocity of the droplets $\mathrm{Ca}_d = \mu V_d/\gamma$ at the centre of the discussion. A third case exists when the channel has a large width/height aspect ratio. This can lead to drops that are strongly confined in only one direction, a situation that has been studied extensively in classical fluid mechanics.[47,48] The flow of such drops and bubbles is very different compared to the above cases. For simplicity, we will restrict our discussion to channels with aspect ratio near one.

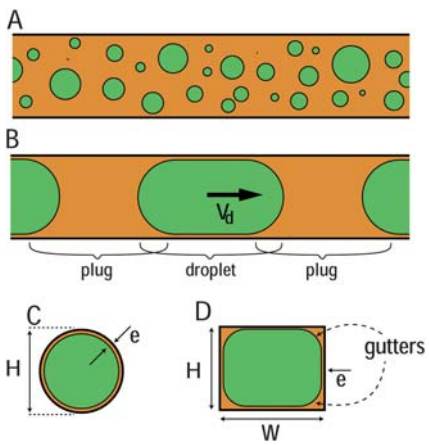

Fig. 4 **A** Dispersed flow: small droplets immersed in a carrier fluid. **B** Slug flow: a succession of plugs and droplets. **C** Cross-section view of a large moving droplet in a circular capillary of diameter H, featuring the thin lubrication film of thickness e. **D** Cross section view of a large moving droplet in a rectangular capillary, featuring thin lubrication films and corners gutters.

In this section we explain the different models for drop transport in microchannels. We assume for simplicity that the carrier fluid completely wets the channel walls, thereby avoiding discussions of contact line dynamics. We also distinguish flows in circular tubes from those in rectangular tubes, which are more relevant to microfluidic situations. Moreover, it is useful to keep in mind that the models of droplet transport can also be understood by focusing on the plugs that separate droplets, which may be easier to address in some cases. Below we concentrate on three aspects of drop transport: the deposition of lubrication films and its relationship to droplet velocity, the pressure drop *vs.* droplet velocity relationships, and the flow patterns that are induced by the immiscible interface.

A. Lubrication films and droplet velocity

Consider a large droplet that is transported in a microchannel, with a velocity V_d from left to right, as depicted in Fig. 4B. As the drop flows, a thin lubrication film of the continuous phase is deposited between the droplet and the channel walls,[49,50] a process that can be understood by balancing viscous entrainment by the channel walls against the capillary pressure in the drop. In the reference frame of the droplet, the channel walls move in the opposite direction with velocity $-V_d$. By viscous entrainment, they pull the carrier fluid from right to left, depositing a "coating film" between the droplet and the walls. On the other hand, the pressure in the droplet is larger than the outside because of the Laplace pressure jump at the interfaces. It therefore pushes against the walls and expels liquid from the deposited films into the bulk. The competition between the viscous drag and capillary pressure determines the thickness e of the lubrication films, which therefore depend on the capillary number Ca_d.

Bretherton[51] found a nonlinear law for e in the case of an inviscid bubble moving at small capillary number in a circular tube of diameter H

$$\frac{e}{H} \propto \mathrm{Ca}_d^{2/3}. \quad (3)$$

Similar scaling results have been derived for moving foams and bubble trains,[52] viscous drops,[53] and extended for any polygonal cross section geometry in the case of a single bubble.[54,55] These

theoretical results have been validated by experiments for circular capillaries[56] and by numerical simulations for both circular and rectangular microchannels.[57,58] These studies confirm that the scaling of eqn (3) holds for $Ca_d < 0.01$. It can therefore be applied to any microfluidic flow, for sufficiently low Ca_d, and it implies that thin films separating drops from the walls will have a thickness on the order of 1% to 5% of the channel's half height.

The presence of lubrication films has a direct implication on the velocity of the droplets; Fairbrother & Stubbs[49] pointed out the general result that, in the reference frame of the droplet, a flux of carrier fluid Q_e can only be accounted for by the difference between the velocity of the droplet V_d and the mean velocity of the carrier fluid V_{ext}, yielding: $Q_e = S\cdot(V_{ext}-V_d)$, where S is the cross-sectional area of the channel. In a circular capillary, the fluid contained in the films is uniformly advected backwards at the wall velocity $-V_d$, such that the drop sees a net flux of the external phase, of magnitude Q_e, which scales with the film thickness: $Q_e \propto -Ca_d^{2/3} S V_d$. As a result, the existence of lubrication films implies that the droplet must move faster than the carrier fluid by an amount

$$\frac{V_d - V_{ext}}{V_d} \propto Ca_d^{2/3}, \tag{4}$$

a relationship that was experimentally verified for circular geometries.[56]

For rectangular microchannels, the picture is modified because the drops do not completely fill the channel's cross section but leave out corner gutters in which the carrier fluid may flow, as shown on Fig. 4D. In their extensive analysis of the problem, Wong *et al.*[55] showed that the gutter flux is in the direction of the bubble's movement and scales as $Q_g \propto Ca_d^{-1/3} S V_d$. It dominates the effect of films by an order in Ca_d, which implies that the droplet velocity is lower than the carrier fluid's by an amount

$$\frac{V_d - V_{ext}}{V_d} \propto -Ca_d^{-1/3}, \tag{5}$$

in agreement with numerical simulations.[59] Nevertheless, the velocity difference should remain below 6% for typical capillary numbers $10^{-6} < Ca_d < 1$.[60]

Fuerstman *et al.*[61] experimentally measured a difference of this magnitude between the droplet and outer fluid velocities. However, they also pointed out that the presence of surfactant can reduce the droplet velocity by up to 50%. These surfactant retardation effects have been observed in other situations[14] and will be treated in Section IVC.

B. Pressure drop and mean velocity

In classical hydraulics and single-phase microfluidics, flows in a uniform straight channel are fully described by a linear compact model which relates the pressure drop ΔP across a channel of length L to the mean flow velocity V:

$$\Delta P = R\cdot L\cdot V = a\frac{\mu}{WH} L\cdot V, \tag{6}$$

where a is a dimensionless constant[61] and R is the fluidic resistivity, analogous to the electrical resistivity in Ohm's law. Such models enable rapid design of electrical or pipe flow networks. Several groups have attempted to develop compact pressure *vs.* flow rate models for microfluidic droplet-laden flows but the physics at play is more delicate.[60–64]

First, the definition of ΔP in eqn (6) is unambiguous for a single-phase Poiseuille flow because the pressure is invariant in the cross-sectional plane of the channel. In the presence of curved immiscible interfaces, care must be taken in defining the path along which the pressure is measured, in order to correctly account for the Laplace pressure jumps. This path can be chosen across the droplet body, thus crossing the front and rear interfaces,[51,54] or directly from plug to plug through the gutters.[61] Here we adopt the first approach which will shed light on the effect of variable curvatures but the two formulations lead to the same result.[55]

As sketched in Fig. 4B, the channel contains a succession of droplets and plugs of carrier fluid, separated by transition regions around the interfaces. The total pressure drop ΔP across the channel is then the sum of the viscous contributions from the plugs ΔP_{plugs} and from the droplets $\Delta P_{droplets}$, in addition to the capillary terms due to the interface curvatures ΔP_{caps}.

Along each plug, the single-phase relation (6) can be used by taking $\mu = \mu_{ext}$ and $V = V_{ext}$, such that the overall pressure drop due to the plugs is

$$\Delta P_{plugs} = a\frac{\mu_f}{WH} L_{plugs}\cdot V_{ext}. \tag{7}$$

The pressure drop due to the interface curvature has only been rigorously studied in the case of an inviscid bubble at small capillary numbers.[51,55] These pressure jumps would compensate if the bubble were symmetric but this symmetry is broken by the motion of the bubble, due to the presence of the lubrication films and spatial variations of their thickness. At the advancing interface the bubble cap is compressed by the liquid that enters the film and therefore has a higher mean curvature. At the rear interface, the exiting fluid expands the interface and lowers the mean curvature. In this way, each bubble introduces a discrete nonlinear pressure drop[51,55] $\Delta P_{caps} \propto Ca_d^{2/3}\gamma/H$, such that the overall pressure drop across the bubbles is[61]

$$\Delta P_{caps} = n_d\cdot c\frac{\gamma}{H} Ca_d^{2/3}, \tag{8}$$

where n_d is the number of bubbles in the channel and c is a dimensionless parameter that depends on geometric parameters (H, W, L_{bubble}). A more detailed treatment of these aspects can be found in a recent review by Ajaev and Homsy.[65] Alternatively, a more intuitive description of the pressure balance across the interface can be obtained by considering the movement of a single plug of liquid that is pushed by a constant pressure.[66,67] This description yields nearly the same physical ingredients, while allowing comparisons with simple experiments in which the plug's length and velocity are independently controlled.

The inviscid theory remains valid for drops of small viscosity ratios $\lambda \ll 1$. Otherwise, Hodges *et al.*[53] have shown that there exists a non-trivial coupling between flows within and outside the drops but that the scaling for the pressure jump at the ends caps ΔP_{caps} still holds. In this case, however, the viscous dissipation inside the droplets is no longer negligible and it is common[60,64] to compute the associated pressure drop $\Delta P_{droplets}$ using the single-phase pressure-flow rate formula of eqn (6), taking $\mu = \mu_{in}$ and

$V = V_d$. Hence, the overall pressure contribution due to a train of viscous droplets is

$$\Delta P_{droplets+caps} = b\frac{\mu_{in}}{WH}L_{droplets} \cdot V_d + n_d \cdot c_\lambda \frac{\gamma}{H}\mathrm{Ca}_d^{2/3}, \quad (9)$$

where b and c_λ are dimensionless parameters that depend on λ and on the geometry.

Finally, the expression of the total pressure drop $\Delta P = \Delta P_{plugs} + \Delta P_{droplets} + \Delta P_{caps}$ is nonlinear, evolves in discrete steps with the number of droplets and involves the velocity of the drops V_d and the mean velocity of the fluid V_{ext}. A sketch of the pressure drop along a channel is shown on Fig. 5, which illustrates the different contributions. We can quantitatively compare each contribution, for example in a flow of inviscid bubbles flowing at $V_{ext} = 1$ mm s^{-1}, in an external fluid with viscosity $\mu_{ext} = 10$ cP, interfacial tension $\gamma = 20$ mN m^{-1} and in a square microchannel with $H = W = 100$ μm. We find that $\Delta P_{plugs} \simeq 100$ Pa/cm, while $\Delta P_{caps} \simeq 10$ Pa per bubble. A density of 10 bubbles/cm would then double the resistance to movement compared with purely viscous effects, even for inviscid bubbles.

However, these pressure *vs.* flow rate relationships are too complex for general use because the constants a, b and c must be re-evaluated when the geometry changes, the relationship with Capillary number breaks down at moderate or high Ca_d,[68] and surfactants greatly modify this simple picture.[61] For this reason, simpler models have been proposed, based on empirical relationships,[63,69] or by considering simplified cases in fixed geometries, such as an inviscid dispersed phase ($\lambda \ll 1$)[60,61] or small droplets.[64] Nonetheless, these nonlinear pressure–flow rate relationships will play a major role in the transport of droplets when the single straight channel is replaced with a network of connected channels. Some of these effects have started to be explored[64,70,71] but much remains to be done in this area.

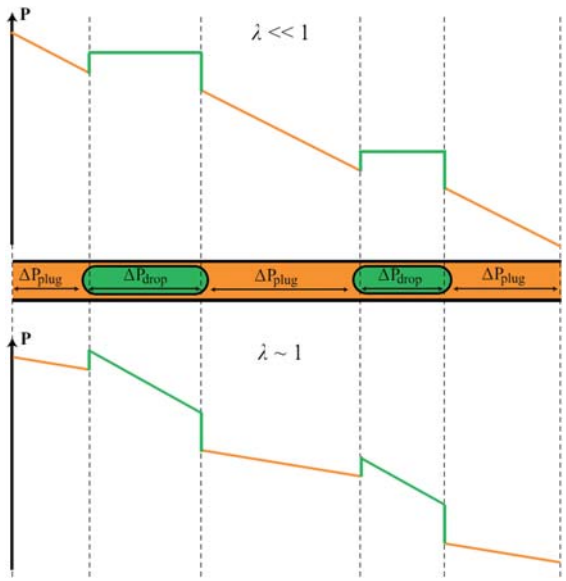

Fig. 5 A qualitative plot of the pressure along a microchannel containing droplets: (top) in the case of an inviscid drop, (bottom) in the case of viscous drops.

C. Flow fields and mixing

A final important aspect of drop transport is related to the flow field induced by the presence of the immiscible interface. In single-phase microfluidics, the base flow has a classic Poiseuille-like profile whose velocity is maximum along the centreline. In the presence of a large drop, this flow field is modified by the fact that the internal and external phases cannot mix. Indeed, the drop travels at a constant velocity V_d which is smaller than the maximum velocity in the external flow. Liquid particles flowing with velocity larger than V_d will therefore catch up with the drop and must change direction when they reach the interface. In the reference frame of the droplet, this translates into the appearance of recirculation zones and stagnation points, *i.e.* points with zero velocity, as shown on Fig. 6.

The same reasoning also applies inside the droplet and it would be mistaken to think that inner fluid moves uniformly at the drop velocity V_d. The correct picture is rather that of a droplet rolling against the side walls like a treadmill. The flow field then corresponds to the Poiseuille-like base flow onto which counter-rotating recirculation rolls are superposed. A qualitative sketch of the flow topology is given in Fig. 6 for a 2-D situation which corresponds to a cut through a circular tube. Even in this simplified configuration, the number and position of recirculation zones depends in a complex manner on the viscosity ratio λ.[53]

The full 3-D flow fields in rectangular microchannels have been visualised by μ-Particle Image Velocimetry,[72,73] by confocal microscopy,[74,75] and through numerical simulations[59] for low-viscosity drops ($\lambda \ll 1$). They reveal features similar to those sketched in Fig. 6A but also point out complex dynamics near the end caps and gutters. Additionally, de Lòzar *et al.*[76] showed in a computational study that the flow fields are highly dependent on the capillary number and the channel's aspect ratio. Nonetheless, the idea of recirculation zones and stagnation points induced by a droplet is a general concept that remains valid and has important implications on transport, mixing and analyte dispersion by the flow.

Concerning the latter, the contents of a drop will remain inside it if the fluids are carefully selected, thus avoiding cross-contamination between droplets. However, the fluid contained in a plug can spread to its neighbours since the droplet acts like a leaky piston, due to the presence of the corner gutters. Nevertheless, the reduction of analyte concentration is weak; it occurs only through the diffusion that carries particles from

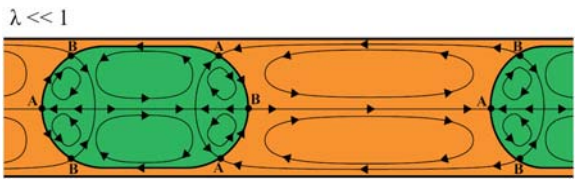

Fig. 6 Topology of the counter-rotating recirculation zones induced by the presence of the interface. The stagnation points on the interface are classified between the converging points A and diverging points B. For non viscous drops, there are 6 recirculation zones inside the droplet and 2 outside. Adapted from Hodges *et al.*[53]

recirculating streamlines to the external streamlines, which remain near the wall.[77]

In terms of mixing, droplet transport always enhances the mixing in both phases compared to single-phase Poiseuille flow, by creating cross-flow advection. This mixing can be inefficient in certain regions of the drop however since the recirculation zones are hydrodynamically isolated from each other. Adding a periodic perturbation to this flow field is sufficient to break the invariant curves that otherwise act as barriers to transport. In that vein, Song *et al.*[3] have used a wavy microchannel to achieve passive homogenisation of droplets in less than 10 ms. An approximate model for this kind of mixing process was given by Stone and Stone.[78] A different approach was demonstrated by Cordero *et al.*[79] who forced a periodic recirculation by creating a time-periodic Marangoni flow induced by alternating laser heating. Furthermore, Gunther *et al.*[72] have shown that wall roughness may even be sufficient to induce chaotic mixing in some cases through slight deformations of the drop geometry.

Finally, understanding the topology of the flow fields is essential to explain effects induced by the remobilisation of surfactants on the interface, such as the retarding mechanism or the modified pressure drop.[80,81] To leading order, we may consider surfactant molecules to be passively advected in the bulk and on the interface by the mean flow, which implies that they must follow the streamlines and can cross them only through molecular diffusion. In addition to this transport, these molecules will adsorb and desorb on the interface with some probability which favours adsorption on average. They are also more likely to adsorb near stagnation points, where the fluid velocity is low and diffusion can act over longer periods. This implies that surfactant molecules will generally be adsorbed on the interface near the converging stagnation points (points **A** on Fig. 6) but they will quickly be transported along the interface away from these points. They will then accumulate near points **B**, where the interface motion concentrates them but where they are trapped by the favourable adsorption.

These mechanisms create a front-to-rear asymmetry which yields a lower value of interfacial tension on the rear *vs.* the front of the droplet. The resulting Marangoni stress can therefore retard the motion of the drop, as explained more quantitatively by Levich[14] in idealised geometries. To this picture one must add the effect of drop deformations, which induce further modifications of the flow field and thus further redistribution of the surfactants. These effects are likely to play a major role in droplet transport but have not yet been elucidated for geometries that are relevant to microfluidics.

D. Local control of transport

Controlling the transport of drops can be done locally, for example in order to select the route that is followed by particular droplets. This implies that an external force must be applied in order to overcome the natural tendency of the drop to follow the surrounding streamlines. Dielectrophoretic forces were first demonstrated to produce such sorting capabilities,[82] with forces in the range of tens of nN. This was shown to be sufficient to select the route that is followed by a drop as it reached a bifurcation, by laterally pushing it across bifurcating streamlines. A similar application of selective routing was also performed by using laser-induced Marangoni flows by Robert de Saint-Vincent *et al.*[83]

More recently, Verneuil *et al.*[84] measured the force that is applied on a drop that is submitted to heating from a focused laser. They found values of several hundred nN, thus explaining the ability to completely block the advance of a drop carried by an external flow. Applications of this opto-thermal control were demonstrated, for example by holding drops stationary in a fluidic "buffer memory", or by switching the order in which they flow.[85] These operations are possible since the scale on which the optical forcing is applied is small compared to the scale of the droplet, contrary to electrical methods which apply an electrical field on a scale larger than the channel size. Finally, Cordero *et al.*[85] showed how variable optical patterns could be used to route drops into three exit channels.

V. Droplet fusion

Efficient use of droplet microfluidics requires drops to be stable against fusion, which is achieved by adding surfactants in the solution.[86] These molecules, which are generally made up of a compact polar head and a long hydrophobic tail, are attracted to the interface separating the drop and the carrier fluid where they align perpendicular to the surface. The surfactant layers on two adjacent drops interact together to retard the merging in several ways: first, they can apply electro-static repulsion between the interfaces, in the case of ionic surfactants. Second, they slow down the hydrodynamic flow along the interface through Marangoni effects or through added surface viscosity. Many of these effects have been extensively studied in the context of foam drainage and emulsions stabilisation (see *e.g.* ref. 86–88), if not in microchannels.

Fusing two drops therefore hinges on overcoming the stabilising effects of the surfactants in order to break the film that separates them. It is usually sufficient to form a localised bridge between two adjacent drops for the merging event to occur, since the local variations in the surface curvature lead to a very rapid "unzipping" of the film, as sketched in Fig. 7a-c. The formation of this liquid bridge leads to a region of the drop with concave curvature, which corresponds to a low pressure region within the droplets. This low pressure draws liquid into the bridge and thus increases its size.

The time taken for the unzipping to occur depends on the magnitude of the pressure decrease and on the resistance to flow.

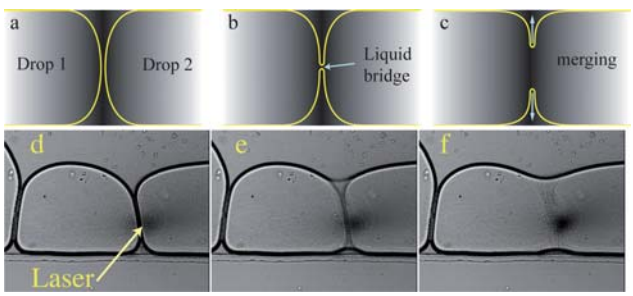

Fig. 7 Sketch of a merging event: a liquid bridge forms between two drops and "unzips" the interfaces to form a new droplet. Experimental sequence showing two drops being merged by localized laser heating. Time between frames is 100 μs.

Modeling for isolated spherical drops[89] predicts a transition between a regime dominated by a capillary-viscous balance and a regime dominated by a capillary-inertia balance. However, the quantitative predictions of such models are difficult to apply in the case of microfluidic drops, since drops in microchannels are almost always confined and their interfaces may depart significantly from a spherical shape. As such, the times predicted for idealised situations should be expected to be far from the actual values observed in a microchannel.

In particular, the effects of confinement may retard the final stages of merging since the lamella of fluid separating the two drops must be drained through a narrow confined space. On the other hand, the merging may be sped up if the interface between the drops is flattened, as in the case of Fig. 7d-f, where the merging event takes place in less than 100 μs. In practice, observations of drop coalescence in microfluidic settings have tended to report merging times of a few hundred microseconds.[90,91]

In recent years, several passive and active methods have been developed for inducing fusion between two droplets. The two approaches have in common the need to first bring the drops into close proximity; this is often done passively, either by modulating the channel geometry in order to slow down the downstream drop until the upstream drop reaches it,[92–94] or by using drops of different sizes which flow at different velocities.[95] Active methods have also been developed for pushing drops into contact, for instance through electro-static attraction by using oppositely charged droplets[96] or by temporarily blocking the motion of a downstream drop with the opto-thermal blocking.[6] Finally, drops have also been captured in double wells in order to co-localise them and induce their fusion while they are stationary.[91]

Once the drops are in close proximity, several merging mechanisms lead to merging through different physical ingredients, as described below.

A. Passive fusion approaches

Bremond *et al.*[93] have measured the moment at which drops merge as they enter a widening then contracting chamber. In this geometry, drops are initially pushed together before getting pulled apart, as shown in Fig. 8(a). Drops are observed to merge while they are being pulled apart, which they term "decompression" merging. This period is also associated with the appearance of pointy structures on the touching drop surfaces, at least in certain cases, and these "nipples" are expected to favour merging by bringing the interfaces closer together and thus inducing the liquid bridge formation. An approximate model is given by Lai *et al.*,[97] who give quantitative predictions for the merging to occur. Note that these nipples also correspond to a rapid increase of the surface area locally and therefore to a temporary reduction of the surfactant concentration at these locations. This variation should also be expected to contribute to the merging of nearby drops, although no measurements of surfactant coverage have been reported. A similar decompression merging was observed to produce an upstream coalescence cascade by Zagnoni *et al.*,[98] who reported the production of long continuous fingers through the merging of a densely packed suspension of droplets.

A different strategy was developed by Niu *et al.*[94] to bring drops into contact and induce their merging. The channel geometry also consisted of a widening section, in order to retard the first drop, but combined this enlargement with the presence of pillars which could completely stop the drop's advance by squeezing its front end. The authors reported observations of decompression merging, as in the case of refs. 93,98, but also of compression merging during which the two drops merged before the downstream drop began to accelerate. It is important to note that no surfactant was added in these experiments, which may explain the ability of drops to merge under compression. Hung *et al.*[92] also observe compressive merging in the absence of surfactant stabilisation.

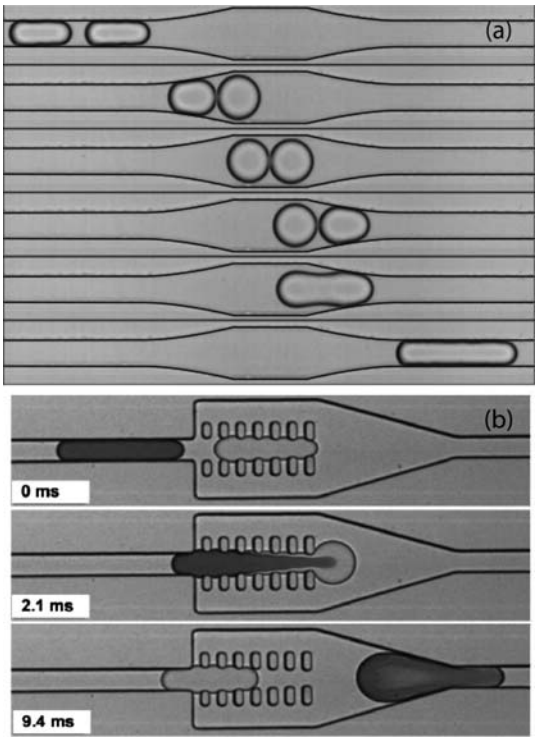

Fig. 8 Geometries for production of passive merging. (a) Decompression merging from Bremond *et al.*[93] and (b) compressive and decompression merging from Niu *et al.*[94] (Image reproduced with permission from Xize Niu, Shelly Gulati, Joshua B. Edel and Andrew J. deMello, Lab Chip, 2008, 8, 1837–1841, ©Royal Society of Chemistry 2008.)

B. Active fusion approaches

Two main approaches have been explored for actively and selectively merging drops. The most widely applied method relies on submitting the drops to an electric field (electrofusion).[90,91,96,98–100] In this case, the drops were observed to reproducibly merge under a very broad set of conditions, with forcing voltages ranging from 1 V to several kV and field frequencies from DC to several kHz. Moreover, fusion was performed using electrodes that were either embedded in the micro-channel or as far away as several mm, with the mean electric fields applied parallel or perpendicular to the touching drop surfaces.

Priest *et al.*[90] interpret the mechanism underlying electrofusion by suggesting that the electric field destabilises a range of capillary waves on the interfaces, which can lead to the formation of

the liquid bridge and the fusion. However, detailed models of the interaction between the electric field and the fluid interfaces are complicated due to the strong feedback between the two. Indeed, the field lines are deviated by the presence of the drops and can be focused into the small lamellae that separate them in the case of dielectric drops, yielding strong field strengths locally. Moreover, the electric field can play a major role in redistributing or reorienting the surfactant molecules, adding further complexity to the problem.

Another approach to fusion is by heating two adjacent droplets with a focused laser.[6,91] The localised heating produces a depletion of the surfactant molecules from the interface, in addition to inducing a complex three-dimensional flow in the fluid.[84] Either of these two mechanisms can lead to the breaking of the lubricating film that separates the two interfaces and by the same token to droplet merging.

It is worth noting here that the large electric fields used to produce electro-fusion and the focusing of field lines also lead to localised temperature increase in the fluids through Joule heating. This could in principle induce surfactant depletion and thermocapillary effects through a similar mechanism to laser heating, although we do not know of any such studies in the literature. However, the use of optical techniques allows finer tuning of the merging position since the heating can be produced on a region that is small compared with the size of the drop, and since the laser focus can be placed at any location in the microchannel.

Finally, an important issue which has not received sufficient attention in the literature is the question of mixing during droplet merging. This problem has been treated for isolated droplets[101] but the confinement in microfluidic channels is likely to play a major role in modifying the behaviour. In particular, although the velocities involved in the merging process are high (roughly 100 μm in 100 μs or 1 m s^{-1}), the dynamics still appears to follow low Reynolds number flows in microfluidics experiments, owing to the small scales and the confinement. Indeed the viscous diffusion time, which determines the time over which viscosity will damp any movement, remains small ($\tau \sim 500$ μs). This means that the velocities observed during the merging process should decay rapidly and that the fluids should lose the memory of the violent event shortly after the merging. The fusion of two droplets containing separate reagents will therefore lead to a sharp interface between the chemical species, as seen for instance in the SI movies of Niu *et al.*[94] where alternating white-black drops are merged. The reaction that occurs between the contents of the two drops can therefore proceed through a reaction-diffusion process[91] or after mixing of the species by the flow.[100]

VI. Summary and discussion

In summary, we have studied the recent progress and current physical knowledge regarding three fundamental droplet operations: Formation, transport, and merging. In each of the cases, certain procedures and microchannel geometries have become standard and are widely used to perform the desired operations. This standardisation provides a reliable set of parameters that allow the applications of droplet microfluidics to advance, for instance in the lab on a chip area. Indeed, the recent explosion of interest in droplets has largely been the product of the pioneering studies that demonstrated fluid combinations, surfactants, forcing methods, and microfluidic geometries that produce reliable operation.

In parallel, the complexity of the behaviour has motivated a large number of fundamental studies aiming to extract the essential elements that govern droplet systems. As shown above, this complexity stems from the deformability of droplets, which introduces nonlinear effects into the otherwise linear Stokes flows. These inherent nonlinearities couple with variations in the channel geometries to produce limitless possible solutions. To this, one must add the very large parameter space of droplet microfluidics; indeed, viscous-capillary interactions can manifest themselves in a wide range of situations and affect the system evolution in unexpected ways. They act both globally, on the scale of the whole drop, or locally on a subregion of the interface. Surfactants and their transport add further complication by inducing surface stresses which modify the flow fields and velocities. Finally, pressure *vs.* flow rate driving can also lead to subtly different flow patterns. For all of these reasons, knowledge of particular flow situations cannot readily be used to predict the behaviour when some of the parameters are changed.

The scope of this review has been limited to hydrodynamic and closely related questions. We have specifically avoided important issues related to physical chemistry of surfaces, which determine in large part the ability to produce drops at all, or compatibility issues of fluids and surfactants. We have also skipped over the exciting recent work on double and multiple emulsions, janus drops, or other complex structures. Finally, we also limited the subject matter to Newtonian fluids, thus overlooking recent work on visco-elastic drop formation.[102] Nonetheless, it is our belief that an intuitive understanding of the underlying hydrodynamics is an important pre-requisite for implementing droplet microfluidics in applications.

Apart from the works cited above, we observe certain emerging areas that will lead to important advances in the near future. In particular, recent publications have touched on the production of two-dimensional arrays of drops,[103–107] motivating studies on the motion of drops in the absence of lateral walls or in the presence of an array of obstacles. Indeed, removing the lateral walls reduces the level of long-range interactions between droplets[108] which simplifies the ability to manipulate them individually.[85] From the point of view of applications, the ability to position particular drops at predetermined locations, *e.g.* in a two-dimensional matrix, yields a significant increase in functionality of droplet-based systems. This approach has been developed by electrowetting or other surface actuation techniques for several years.[10] However, interfacing such a two-dimensional device with a microchannel system for drop formation and preconditioning would bridge the gap between microchannel-based systems and digital microfluidics on surfaces, thus taking advantage of the qualities of both approaches.

Acknowledgements

The authors acknowledge useful discussions with Maria-Luisa Cordero. We thank Sungyon Lee, Howard Stone, and Todd

Squires for careful reading of the manuscript and useful feedback.

References

1 P. B. Umbanhowar, V. Prasad and D. A. Weitz, Monodisperse emulsion generation *via* drop break off in a coflowing stream, *Langmuir*, 2000, **16**, 347–351.
2 A. S. Utada, E. Lorenceau, D. R. Link, P. D. Kaplan, H. A. Stone and D. A. Weitz, Monidisperse double emulsions generated from a microcapillary device, *Science*, 2005, **308**, 537–541.
3 H. Song, J. D. Tice and R. F. Ismagilov, A microfluidic system for controlling reaction networks in time, *Angew. Chem., Int. Ed.*, 2003, **42**(7), 768–772.
4 B. Rotman, Measurement of activity of single molecules of β-D-galactosidase, *Proc. Natl. Acad. Sci.*, 1981, **47**(12), 1961.
5 D. S. Tawfik and A. D. Griffiths, Man-made cell-like compartments for molecular evolution, *Nat. Biotechnol.*, 1998, **16**, 652–656.
6 C. N. Baroud, M. R. de Saint Vincent and J.-P. Delville, An optical toolbox for total control of droplet microfluidics, *Lab Chip*, July 2007, **7**, 1029–1033.
7 J. P. Raven and P. Marmottant, Periodic microfluidic bubbling oscillator: Insight into the stability of two-phase microflows, *Phys. Rev. Lett.*, 2006, **97**(15), 154501.
8 P. Guillot, A. Colin, A. S. Utada and A. Ajdari, Stability of a jet in confined pressure-driven biphasic flows at low reynolds numbers, *Phys. Rev. Lett.*, 2007, **99**, 104502.
9 P. Huerre and P. A. Monkewitz, Local and global instabilities in spatially developing flows, *Annu. Rev. Fluid Mech.*, 1990, **22**(1), 473–537.
10 A. A. Darhuber and S. M. Troian, Principles of microfluidic actuation by modulation of surface stresses, *Annu. Rev. Fluid Mech.*, 2005, **37**, 425–455.
11 G. I. Taylor, The formation of emulsions in definable fields of flow, *Proc. R. Soc. London, Ser. A*, 1934, **146**, 501–523.
12 D. R. Link, S. L. Anna, D. A. Weitz and H. A. Stone, Geometrically mediated breakup of drops in microfluidic devices, *Phys. Rev. Lett.*, 2004, **92**(5), 054503.
13 L. Ménétrier-Deremble and P. Tabeling, Droplet breakup in microfluidic junctions of arbitrary angles, *Phys. Rev. E*, 2006, **74**, 035303.
14 V. G. Levich. *Physicochemical Hydrodynamics*. Prentice Hall, Englewood Clifs, N. J., 1962. Chapters 7 and 8.
15 C. D. Eggleton, T.-M. Tsai and K. J. Stebe, Tip streaming from a drop in the presence of surfactants, *Phys. Rev. Lett.*, 2001, **87**, 048302, –1–4.
16 H. A. Stone and L. G. Leal, The effects of surfactants on drop deformation and breakup, *J. Fluid Mech.*, 1990, **220**, 161–186.
17 G. F. Christopher and S. L. Anna, Microfluidic methods for generating continuous droplet streams, *J. Phys. D: Appl. Phys.*, 2007, **40**, R319–R336.
18 C. Cramer, P. Fischer and E. J. Windhab, Drop formation in a co-flowing ambient fluid, *Chem. Eng. Sci.*, 2004, **59**(15), 3045–3058.
19 A. S. Utada, A. Fernandez-Nieves, H. A. Stone and D. A. Weitz, Dripping to jetting transitions in coflowing liquid streams, *Phys. Rev. Lett.*, 2007, **99**, 094502.
20 A. S. Utada, A. Fernandez-Nieves, J. M. Gordillo and D. A. Weitz, Absolute instability of a liquid jet in a coflowing stream, *Phys. Rev. Lett.*, 2008, **100**, 014502.
21 P. Guillot, A. Colin and A. Ajdari, Stability of a jet in confined pressure-driven biphasic flows at low Reynolds number in various geometries, *Phys. Rev. E*, 2008, **78**(1, Part 2).
22 K. B. Migler, String formation in sheared polymer blends: Coalescence, breakup, and finite size effects, *Phys. Rev. Lett.*, 2001, **86**(6), 1023–1026.
23 K. J. Humphry, A. Ajdari, A. Fernández-Nieves, H. A. Stone and D. A. Weitz, Suppression of instabilities in multiphase flow by geometric confinement, *Phys. Rev. E*, 2009, **79**(5), 56310.
24 T. Thorsen, R. W. Roberts, F. H. Arnold and S. R. Quake, Dynamic pattern formation in a vesicle-generating microfluidic device, *Phys. Rev. Lett.*, 2001, **86**(18), 4163–4166.
25 P. Garstecki, M. J. Fuerstman, H. A. Stone and G. M. Whitesides, Formation of droplets and bubbles in a microfluidic T-junction. scaling and mechanism of break-up, *Lab Chip*, 2006, **6**(3), 437–446.
26 M. de Menech, P. Garstecki, F. Jousse and H. A. Stone, Transition from squeezing to driipping in a microfluidic T-shaped junction, *J. Fluid Mech.*, 2008, **595**, 141–161.
27 P. Guillot and A. Colin, Stability of parallel flows in a microchannel after a T junction, *Phys. Rev. E.*, 2005, **72**(6), 66301.
28 M. De Menech, Modeling of droplet breakup in a microfluidic t-shaped junction with a phase-field model, *Phys. Rev. E.*, 2006, **73**, 031505.
29 V. van Steijn, M. T. Kreutzer and C. R. Kleijn, μ-PIV study of the formation of segmented flow in microfluidic T-junctions, *Chem. Eng. Sci.*, 2007, **62**(24), 7505–7514.
30 G. F. Christopher, N. N. Noharuddin, J. A. Taylor and S. L. Anna, Experimental observations of the squeezing-to-dripping transition in t-shaped microfluidic junctions, *Phys. Rev. E.*, 2008, **78**(3), 036317.
31 V. van Steijn, C. R. Kleijn and M. T. Kreutzer, Flows around confined bubbles and their importance in triggering pinch-off, *Phys. Rev. Lett.*, 2009, **103**(21), 214501.
32 S. L. Anna, N. Bontoux and H. A. Stone, Formation of dispersions using flow-focusing' in microchannels, *Appl. Phys. Lett.*, 2003, **82**(3), 364–366.
33 R. Dreyfus, P. Tabeling and H. Willaime, Ordered and discordered patterns in two phase flows in microchannels, *Phys. Rev. Lett.*, 2003, **90**, 144505.
34 P. Garstecki, H. A. Stone and G. M. Whitesides, Mechanism for flow-rate controlled breakup in confined geometries: A route to monodisperse emulsions, *Phys. Rev. Lett.*, 2005, **94**, 164501.
35 B. Dollet, W. van Hoeve, J. P. Raven, P. Marmottant and M. Versluis, Role of the channel geometry on the bubble pinch-off in flow-focusing devices, *Phys. Rev. Lett.*, 2008, **100**(3), 034504.
36 T. Cubaud and T. G. Mason, Capillary threads and viscous droplets in square microchannels, *Phys. Fluids*, 2008, **20**, 053302.
37 W. Lee, L. M. Walker and S. L. Anna, Role of geometry and fluid properties in droplet and thread formation processes in planar flow focusing, *Phys. Fluids*, 2009, **21**, 032103.
38 T. Ward, M. Faivre, M. Abkarian and H. A. Stone, Microfluidic flow focusing: Drop size and scaling in pressure *versus* flow-rate-driven pumping, *Electrophoresis*, 2005, **26**, 3716–3724.
39 D. Funfschilling, H. Debas, H. Z. Li and T. G. Mason, Flow-field dynamics during droplet formation by dripping in hydrodynamic-focusing microfluidics, *Phys. Rev. E.*, 2009, **80**(1), 15301.
40 H. Willaime, V. Barbier, L. Kloul, S. Maine and P. Tabeling, Arnold Tongues in a Microfluidic Drop Emitter, *Phys. Rev. Lett.*, 2006, **96**(5), 54501.
41 S. Zeng, B. Li, X. Su, J. Qin and B. Lin, Microvalve-actuated precise control of individual droplets in microfluidic devices, *Lab Chip*, 2009, **9**(10), 1340–1343.
42 J. C. Galas, D. Bartolo and V. Studer, Active connectors for microfluidic drops on demand, *New J. Phys.*, 2009, **11**(075027).
43 C. N. Baroud, J. P. Delville, F. Gallaire and R. Wunenburger, Thermocapillary valve for droplet production and sorting, *Phys. Rev.E*, 2007, **75**(4), 046302.
44 N. T. Nguyen, T. H. Ting, Y. F. Yap, T. N. Wong, J. C. K. Chai, W. L. Ong, J. Zhou, S. H. Tan and L. Yobas, Thermally mediated droplet formation in microchannels, *Appl. Phys. Lett.*, 2007, **91**, 084102.
45 C. A. Stan, S. K. Y. Tang and G. M. Whitesides, Independent Control of Drop Size and Velocity in Microfluidic Flow-Focusing Generators Using Variable Temperature and Flow Rate., *Anal. Chem.*, 2009, **81**(6), 2399–2402.
46 Y.-C. Tan, J. S. Fisher, A. I. Lee, V. Cristini and A. P. Lee, Design of microfluidic channel geometries for the control of droplet volume, chemical concentration, and sorting, *Lab Chip*, 2004, **4**, 292–298.
47 P. G. Saffman and G. I. Taylor, The penetration of a fluid into a porous medium or hele-shaw cell containing a more viscous liquid, *Proc. R. Soc. London, Ser. A*, 1958, **245**, 312–329.
48 A. R. Kopf-Sill and G. M. Homsy, Bubble motion in a Hele–Shaw cell, *Phys. Fluids*, 1988, **31**, 18.
49 F. Fairbrother and A. E. Stubbs, Studies in electroendosmosis. part vi. the bubble-tube methods of measurement, *J. Chem. Soc.*, 1935.
50 G. I. Taylor, Deposition of a viscous fluid on the wall of a tube, *J. Fluid Mech.*, 1961, **10**, 161–165.
51 F. P. Bretherton, The motion of long bubbles in tubes, *J. Fluid Mech.*, 1961, **10**, 166–188.
52 J. Ratulowski and H.-C. Chang, Transport of gas bubbles in capillaries, *Phys. Fluids A*, 1989, **1**(10), 1642–1655.

53 S. R. Hodges, O. E. Jensen and J. M. Rallison, The motion of a viscous drop through a cylindrical tube, *J. Fluid Mech.*, 2004, **501**, 279–301.
54 H. Wong, C. J. Radke and S. Morris, The motion of long bubbles in polygonal capillaries. part 1. thin films, *J. Fluid Mech.*, 1995, **292**, 71–94.
55 H. Wong, C. J. Radke and S. Morris, The motion of long bubbles in polygonal capillaries. part 2. drag, fluid pressure and fluid flow, *J. Fluid Mech.*, 1995, **292**, 95–110.
56 L. W. Schwartz, H. M. Princen and A. D. Kiss, On the motion of bubbles in capillary tubes, *J. Fluid Mech.*, 1986, **172**, 259–275.
57 D. A. Reinelt and P. G. Saffman, The penetration of a finger into a viscous fluid in a channel and tube, *SIAM J. Sci. Stat. Comput.*, 1985, **6**, 542–561.
58 A. L. Hazel and M. Heil, The steady propagation of a semi-infinite bubble into a tube of elliptical or rectangular cross-section, *J. Fluid Mech.*, 2002, **470**, 91–114.
59 F. Sarrazin, T. Bonometti, L. Prat, C. Gourdon and J. Magnaudet, Hydrodynamic structures of droplets engineered in rectangular micro-channels, *Microfluid. Nanofluid.*, 2008, **5**, 131–137.
60 F. Jousse, G. P. Lian, R. Janes and J. Melrose, Compact model for multi-phase liquid–liquid flows in micro-fluidic devices, *Lab Chip*, 2005, **5**(6), 646–656.
61 M. J. Fuerstman, A. Lai, M. E. Thurlow, S. S. Shevkoplyas, H. A. Stone and G. M. Whitesides, The pressure drop along rectangular microchannels containing bubbles, *Lab Chip*, 2007, **7**(11), 1479–1489.
62 M. Schindler and A. Ajdari, Droplet traffic in microfluidic networks: A simple model for understanding and designing, *Phys. Rev. Lett.*, 2008, **100**(4), 044501.
63 V. Labrot, M. Schindler, P. Guillot, A. Colin and M. Joanicot, Extracting the hydrodynamic resistance of droplets from their behavior in microchannel networks, *Biomicrofluidics*, 2009, **3**, 012804.
64 D. A. Sessoms, M. Belloul, W. Engl, M. Roche, L. Courbin and P. Panizza, Droplet motion in microfluidic networks: Hydrodynamic interactions and pressure-drop measurements, *Phys. Rev. E.*, 2009, **80**(1), 016317.
65 V. S. Ajaev and G. M. Homsy, Modeling shapes and dynamics of confined bubbles, *Annu. Rev. Fluid Mech.*, 2006, **38**(1), 277–307.
66 J. Bico and D. Quéré, Falling slugs, *J. Colloid Interface Sci.*, 2001, **243**, 262–264.
67 C. P. Ody, C. N. Baroud, and E. de Langre. Transport of wetting liquid plugs in bifurcating microfluidic channels. *J. Colloid Interface Sci.*, 308:pp. 231–238, Jan. 2007.
68 S. A. Vanapalli, A. G. Banpurkar, D. Ende, M. H. G. Duits and F. Mugele, Hydrodynamic resistance of single confined moving drops in rectangular microchannels, *Lab Chip*, 2009, **9**(7), 982–990.
69 B. J. Adzima and S. S. Velankar, Pressure drops for droplet flows in microfluidic channels, *J. Micromech. Microeng.*, 2006, **16**(8), 1504–1510.
70 W. Engl, M. Roche, A. Colin, P. Panizza and A. Ajdari, Droplet Traffic at a Simple Junction at Low Capillary Numbers, *Phys. Rev. Lett.*, 2005, **95**(20), 208304.
71 M. Prakash and N. Gershenfeld, Microfluidic bubble logic, *Science*, 2007, **315**, 832–835.
72 A. Günther, M. Jhunjhunwala, M. Thalmann, M. A. Schmidt and K. F. Jensen, Micromixing of Miscible Liquids in Segmented Gas-Liquid Flow, *Langmuir*, 2005, **21**(4), 1547–1555.
73 F. Sarrazin, L. Prat, N. Di Miceli, G. Cristobal, D. R. Link and D. A. Weitz, Mixing characterization inside microdroplets engineered on a microcoalescer, *Chem. Eng. Sci.*, 2007, **62**, 1042–1048.
74 H. Kinoshita, S. Kaneda, T. Fujii and M. Oshima, Three-dimensional measurement and visualization of internal flow of a moving droplet using confocal micro-piv, *Lab Chip*, 2007, **7**, 338–346.
75 R. Lindken, M. Rossi, S. Große and J. Westerweel, Micro-Particle Image Velocimetry (μPIV): Recent developments, applications, and guidelines, *Lab Chip*, 2009, **9**(17), 2551–2567.
76 A. de Lózar, A. L. Hazel and A. Juel, Scaling properties of coating flows in rectangular channels, *Phys. Rev. Lett.*, 2007, **99**(23), 234501.
77 M. T. Kreutzer, A. Gunther and K. F. Jensen, Sample Dispersion for Segmented Flow in Microchannels with Rectangular Cross Section, *Anal. Chem.*, 2008, **80**(5), 1558–1567.
78 Z. B. Stone and H. A. Stone, Imaging and quantifying mixing in a model droplet micromixer, *Phys. Fluids*, 2005, **17**, 063103.
79 M. L. Cordero, H. O. Rolfsnes, D. R. Burnham, P. A. Campbell, D. McGloin and C. N. Baroud, Mixing *via* thermocapillary generation of flow patterns inside a microfluidic drop, *New J. Phys.*, 2009, **11**, 075033.
80 K. J. Stebe, S. Y. Lin and C. Maldarelli, Remobilizing surfactant retarded fluid particle interfaces. I. Stress-free conditions at the interfaces of micellar solutions of surfactants with fast sorption kinetics, *Phys. Fluids A: Fluid Dynamics*, 1991, **3**, 3.
81 K. J. Stebe and C. Maldarelli, Remobilizing Surfactant Retarded Fluid Particle Interfaces:: II. Controlling the Surface Mobility at Interfaces of Solutions Containing Surface Active Components, *J. Colloid Interface Sci.*, 1994, **163**(1), 177–189.
82 K. Ahn, C. Kerbage, T. Hynt, R. M. Westervelt, D. R. Link and D. A. Weitz, Dielectrophoretic manipulation of drops for high-speed microfluidic sorting devices, *Appl. Phys. Lett.*, 2006, **88**, 024104.
83 M. Robert de Saint Vincent, R. Wunenburger and J. P. Delville, Laser switching and sorting for high speed digital microfluidics, *Appl. Phys. Lett.*, 2008, **92**(15), 154105.
84 E. Verneuil, M. L. Cordero, F. Gallaire and C. N. Baroud, Laser-induced force on a microfluidic drop: Origin and magnitude, *Langmuir*, 2009, **25**(9), 5127–5134.
85 M. L. Cordero, D. R. Burnham, C. N. Baroud and D. McGloin, Thermocapillary manipulation of droplets using holographic beam shaping: Microfluidic pin ball, *Appl. Phys. Lett.*, 2008, **93**(3), 034107.
86 J. Bibette, D. C. Morse, T. A. Witten and D. A. Weitz, Stability criteria for emulsions, *Phys. Rev. Lett.*, 1992, **69**, 2439–2442.
87 Y. Amarouchene, G. Cristobal and H. Kellay, Noncoalescing drops, *Phys. Rev. Lett.*, 2001, **87**, 206104.
88 A. Saint-Jalmes, Y. Zhang and D. Langevin, Quantitative description of foam drainage: Transitions with surface mobility, *Eur. Phys. J. E*, 2004, **15**, 53–60.
89 J. Eggers, J. R. Lister and H. A. Stone, Coalescence of liquid drops, *J. Fluid Mech.*, 1999, **401**, 293–310.
90 C. Priest, S. Herminghaus and R. Seemann, Controlled electrocoalescence in microfluidics: Targeting a single lamella, *Appl. Phys. Lett.*, 2006, **89**, 134101.
91 A. Huebner, C. Abell, W. T. S. Huck, C. N. Baroud, and F. Hollfelder. Triggered fusion of picolitre droplets: monitoring a reaction at sub-millisecond resolution. Submitted.
92 L. H. Hung, K. M. Choi, W. Y. Tseng, Y. C. Tan, K. J. Shea and A. P. Lee, Alternating droplet generation and controlled dynamic droplet fusion in microfluidic device for CdS nanoparticle synthesis, *Lab Chip*, 2006, **6**(2), 174–178.
93 N. Bremond, A. R. Thiam and J. Bibette, Decompressing emulsion droplets favors coalescence, *Phys. Rev. Lett.*, 2008, **100**(2), 024501.
94 X. Niu, S. Gulati, J. B. Edel and A. J. deMello, Pillar-induced droplet merging in microfluidic circuits, *Lab Chip*, 2008, **8**(11), 1837–1841.
95 L. Mazutis, J. C. Baret, P. Treacy, Y. Skhiri, A. F. Araghi, M. Ryckelynck, V. Taly and A. D. Griffiths, Multi-step microfluidic droplet processing: kinetic analysis of an in vitro translated enzyme, *Lab Chip*, 2009, **9**(20), 2902–2908.
96 D. R. Link, E. Grasland-Mongrain, A. Duri, F. Sarrazin, Z. Cheng, G. Cristobal, M. Marquez and D. A. Weitz, Electric control of droplets in microfluidic devices, *Angew. Chem., Int. Ed.*, 2006, **45**(16), 2556–2560.
97 A. Lai, N. Bremond and H. A. Stone, Separation-driven coalescence of droplets: an analytical criterion for the approach to contact, *J. Fluid Mech.*, 2009, **632**, 97–107.
98 M. Zagnoni, C. N. Baroud and J. M. Cooper, Electrically initiated upstream coalescence cascade of droplets in a microfluidic flow, *Phys. Rev. E.*, 2009, **80**(4), 046303.
99 M. Chabert, K. D. Dorfman and J. L. Viovy, Droplet fusion by alternating current (AC) field electrocoalescence in microchannels, *Electrophoresis*, 2005, **26**, 3706–3715.
100 K. Ahn, J. Agresti, H. Chong, M. Marquez and D. A. Weitz, Electrocoalescence of drops synchronized by size-dependent flow in microfluidic channels, *Appl. Phys. Lett.*, 2006, **88**, 264105.
101 A. V. Anilkumar, C. P. Lee and T. G. Wang, Surface-tension-induced mixing following coalescence of initially stationary drops, *Phys. Fluids A: Fluid Dynamics*, 1991, **3**, 2587–2591.

102 P. E. Arratia, J. P. Gollub and D. J. Durian, Polymeric filament thinning and breakup in microchannels, *Phys. Rev. E*, 2008, **77**(3), 36309.
103 J. Shim, G. Cristobal, D. R. Link, T. Thorsen, Y. Jia, K. Piattelli and S. Fraden, Control and Measurement of the Phase Behavior of Aqueous Solutions Using Microfluidics, *J. Am. Chem. Soc.*, 2007, **129**(28), 8825–8835.
104 W. Shi, J. Qin, N. Ye and B. Lin, Droplet-based microfluidic system for individual Caenorhabditis elegans assay, *Lab Chip*, 2008, **8**(9), 1432–1435.
105 A. Huebner, D. Bratton, G. Whyte, M. Yang, A. J. deMello, C. Abell and F. Hollfelder, Static microdroplet arrays: a microfluidic device for droplet trapping, incubation and release for enzymatic and cell-based assays, *Lab Chip*, 2009, **9**(5), 692–698.
106 H. Kim, S. Vishniakou and G. W. Faris, Petri dish PCR: laser-heated reactions in nanoliter droplet arrays, *Lab Chip*, 2009, **9**(9), 1230–1235.
107 L. Mugherli, O. N. Burchak, L. A. Balakireva, A. Thomas, F. Chatelain and M. Y. Balakirev, In situ assembly and screening of enzyme inhibitors with surface-tension microarrays, *Angew. Chem., Int. Ed.*, 2009, 1433–7851.
108 T. Beatus, T. Tlusty and R. Bar-Ziv, Phonons in a one-dimensional microfluidic crystal, *Nat. Phys.*, 2006.